



UNIVERSITY OF LEEDS

This is a repository copy of *Lead Sulfide (PbS) Scale Behavior and Deposition as a Function of Polymeric Sulfide Inhibitor Concentration in Multiphase*.

White Rose Research Online URL for this paper:
<http://eprints.whiterose.ac.uk/131039/>

Version: Accepted Version

Proceedings Paper:

Keogh, W, Boakye, GO, Neville, A orcid.org/0000-0002-6479-1871 et al. (8 more authors) (2018) Lead Sulfide (PbS) Scale Behavior and Deposition as a Function of Polymeric Sulfide Inhibitor Concentration in Multiphase. In: NACE 2018: Proceedings of the International Corrosion Conference and Expo Series. NACE CORROSION 2018 Conference and Expo, 15-19 Apr 2018, Phoenix, Arizona, USA. National Association of Corrosion Engineers .

(c) 2018. NACE International. This is an author produced version of a paper published in NACE 2018: Proceedings of the International Corrosion Conference and Expo Series. Uploaded in accordance with the publisher's self-archiving policy.

Reuse

Items deposited in White Rose Research Online are protected by copyright, with all rights reserved unless indicated otherwise. They may be downloaded and/or printed for private study, or other acts as permitted by national copyright laws. The publisher or other rights holders may allow further reproduction and re-use of the full text version. This is indicated by the licence information on the White Rose Research Online record for the item.

Takedown

If you consider content in White Rose Research Online to be in breach of UK law, please notify us by emailing eprints@whiterose.ac.uk including the URL of the record and the reason for the withdrawal request.



eprints@whiterose.ac.uk
<https://eprints.whiterose.ac.uk/>

Lead Sulfide (PbS) Scale Behavior and Deposition as a Function of Polymeric Sulfide Inhibitor Concentration in Multiphase

William Keogh, Gifty Oppong Boakye, Anne Neville
Institute of Functional Surfaces (IFS)
University of Leeds
Leeds, LS2 9JT
England

Thibaut Charpentier
School of Chemical and Process Engineering
University of Leeds
Leeds, LS2 9JT
England

John Helge Olsen
Statoil ASA
4035
Stavanger
Norway

Violette Eroini
Statoil ASA
5020
Bergen
Norway

Frank Møller Nielsen
Statoil ASA
7053
Trondheim
Norway

Jon Ellingsen, Oeystein Bache
ConocoPhillips
4056
Stavanger
Norway

Salima Baraka-Lokmane
TOTAL
64000
Pau
France

Etienne Bourdelet
TOTAL
4029
Stavanger
Norway

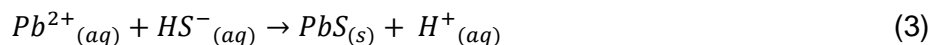
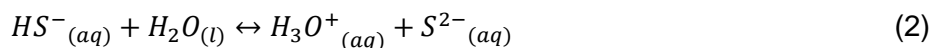
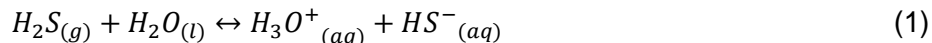
ABSTRACT

Deposition of inorganic mineral scale on downhole completion equipment contributes to significant downtime and loss of production within the oil and gas industry. High temperature/high pressure (HT/HP) fields have reported build-up of lead sulfide (PbS) scale as a consequence of reservoir souring; and the resultant reaction between dissociated sulfide anions from hydrogen sulfide (H₂S) and heavy metal cations. In this work, laboratory apparatus enabled simulation of scale precipitation under turbulent emulsion-forming multiphase conditions, with behavior of PbS particles at the oil/water interface and subsequent adhesion onto anti-fouling surfaces measured at a range of polymer concentrations. Introduction of polymer sulfide inhibitor (PSI) product to the formation brine at concentrations of 500mg/L reduced overall PbS deposition whilst addition of 5000mg/L further reduced scale crystallisation but resulted in complete emulsification of the light oil phase. The tendency of soluble polymers to act as surfactants led to increased stabilisation of the formed oil in water (o/w) emulsion with heightened PSI concentration. Optical microscope, gravimetric and rheological measurements explained depositional behaviour; whereby enhanced o/w emulsion viscosity and stability due to amphiphilic polymer adsorption onto both PbS scale and oil droplet interfaces resulted in uniform deposition upon all surfaces.

Key words: mineral scale, lead sulfide, Pickering emulsion, anti-fouling, polymeric inhibitor

INTRODUCTION

Evolution of H₂S gas within oil reservoirs can occur through both microbiological and geochemical means; a consequence of the activity of Sulfate Reducing Bacteria (SRB) and chemical reactions resulting from seawater injection, respectively ¹. The dissociation of H₂S to its constituent anions in water can be seen in equations 1 and 2, with Pb²⁺ cations within produced water reacting readily with sulfide based species to form PbS (galena), as seen in equation 3.



Flow assurance complications in oil and gas production associated with deposition of sulfide scales are becoming increasingly frequent in high temperature/high pressure (HT/HP) fields. This paper builds on previous work ^{2, 3}, where adhesion of PbS nanoparticles onto surfaces was found to be the overwhelmingly dominant deposition mechanism; with fouling behavior contingent on formation of an oil in water (o/w) Pickering emulsion and wettability of the foreign surface in a multiphase system. As such, oil wetted hydrophobic fluoropolymer surfaces were found to significantly limit the adhesion of PbS scale ². Whilst the scaling mitigation potential of both anti-fouling surfaces and inhibitors has been investigated extensively on an individual basis ⁴⁻⁷, this work is the first on their combined efficacy in sulfide forming multiphase processes. As operators become increasingly intent on applying anti-fouling coatings onto downhole equipment to prevent the deposition and build-up of scales, understanding the synergy (or lack thereof) between chemical and surface mitigation techniques is critical.

Polymers, utilised in the removal of heavy metal cations from aqueous solutions, are commonly implemented in industrial applications such as wastewater treatment, as well as chemical inhibition of inorganic scale growth in oilfield systems ^{6, 8}. The amphiphilic nature of the polymeric sulfide inhibitor (PSI) allows both inhibition of crystal nucleation through cation complexation, and growth retardation after adsorption upon crystalline surfaces ⁹. Water-soluble polymers also behave as surfactants and are used in a multitude of applications related to emulsion stabilization; such as gene and drug delivery, detergents, ceramics etc. In oil and gas production, chemically enhanced oil recovery (CEOR) is driven by adsorption of viscosity enhancing polymers at the o/w interface, with performance influenced by aqueous pH, block structure and length, and concentration ¹⁰.

In this contribution, a novel apparatus introduced H₂S gas into the air-space of an anaerobic reaction vessel, where it gradually diffused into the aqueous Pb²⁺ cation rich brine phase before reaching equilibrium and dissociating into reactive bisulfide (HS⁻) species. The experimental procedure reflected mechanisms and conditions present during production within a sulfide forming well, where aqueous H₂S concentrations can reach up to 55 ppm at equilibrium; and turbulent, two-phase flow conditions are generated in an anaerobic environment at pH 5-6 ¹¹⁻¹³. An o/w emulsion was established by the bulk aqueous and light oil phases present within the system, modeling turbulent multiphase flow within a production tubing line at the interface of tested anti-fouling surfaces. A range of analytical techniques were then used to determine the effect of PSI concentration on PbS precipitation and emulsion behavior, and subsequently ascertain how deposition upon anti-fouling surfaces was influenced.

EXPERIMENTAL PROCEDURE

Anti-fouling surfaces

Three promising anti-fouling coatings applied to industry standard steel (UNS N07718) 12mm (0.472 in) diameter cylindrical coupons were tested alongside an uncoated sample. Fluoropolymer surfaces F1 and F2 were hydrophobic in nature, while conversely DLC and REF were hydrophilic, as seen in Table 1.

Table 1
Anti-fouling coatings and properties

| Coating | Water contact angle (°) | Coating type |
|---------|-------------------------|-------------------------|
| F1 | 101 | Fluoropolymer |
| F2 | 103 | |
| DLC | 68 | Diamond-like carbon |
| REF | 71 | UNS N07718 steel (none) |

Experimental set-up

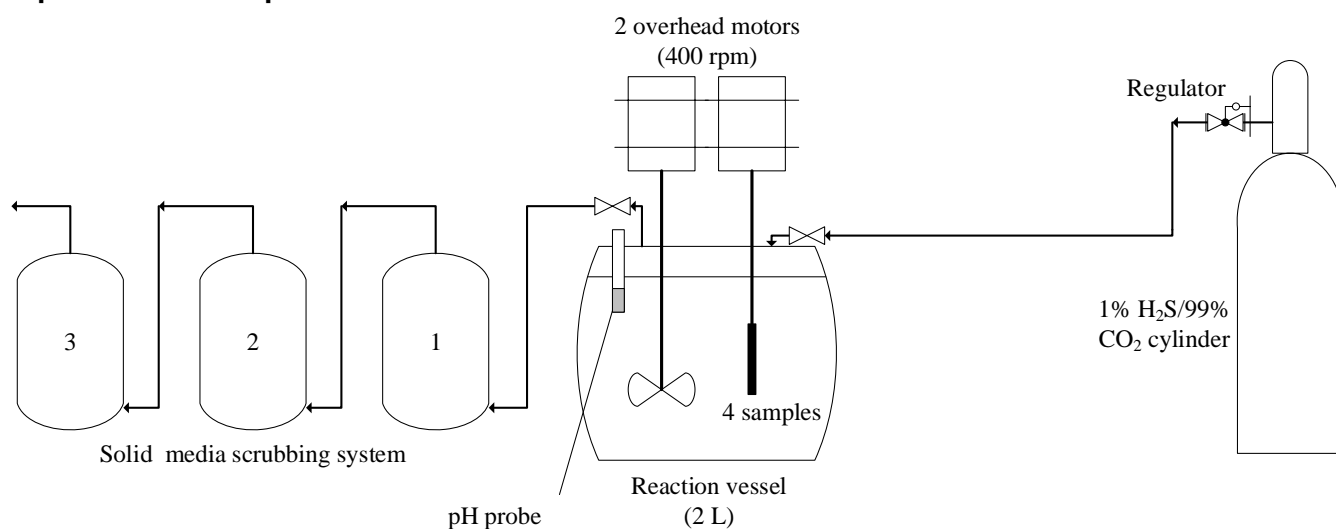


Figure 1: Schematic of experimental scaling rig

Figure 1 shows a schematic of the equipment, whereby a gas blend of 1% H₂S/99% CO₂ entered a 2 liter (L) reaction vessel under anaerobic conditions. Fed into the gaseous phase, H₂S and CO₂ diffused into the brine and subsequently dissociated/became hydrolyzed respectively. A bladed impeller connected to an overhead motor emulsified the oil and water phases, with 4 samples correspondingly rotated at 400 RPM to create turbulence at the coating interfaces. Excess gas was fed into an activated carbon/alumina scrubbing system to remove H₂S from the flow stream.

Scaling test

A lead (II) chloride (PbCl₂) brine was formulated and stirred thoroughly for 1 hour in 1900 mL of distilled water to fully dissolve the PbCl₂ salt, with 100 mL of synthetic distillate introduced to form a ratio of 95:5 (v/v) water:oil up to 2 L. Addition of 1.35 g/L of PbCl₂ salt to the brine solution resulted in a Pb²⁺ concentration of 1000 mg/L with an initial saturation ratio (SR_{initial}) of 1.5x10²², prompting spontaneous nucleation of PbS within the aqueous phase. 50 mL of acetic acid buffer (48 mL 5M acetic acid and 452 mL of 5M sodium acetate in 1 L distilled water) was used to make up the PbCl₂ brine, and was used to maintain a constant pH of 5.2 within the reaction vessel, preventing pH reduction within a closed system. This promoted formation of reactive HS⁻ anions throughout the experiment whilst keeping the pH stable,

monitored by a pH probe, at levels expected within a sour production well. Tests were run at three PSI concentrations (product) of 0, 500 and 5000 mg/L (v/v), added to the PbCl₂ brine before the experiment was initiated.

Tests were run within an airtight reaction vessel, initially sparged with carbon dioxide (CO₂) gas for a period of 2 hours to ensure anaerobic conditions during testing, preventing the formation of sulfates. Gas in a blend of 1% H₂S/99% CO₂ was then introduced into the air phase of the reaction vessel at a constant pressure of 1.1-1.2 bar (absolute), controlled via a regulator connected to a pressurized cylinder (Figure 1). Under these conditions, H₂S concentration reached approximately 30 ppm in the aqueous phase at equilibrium. Due to the toxicity of H₂S gas, all experiments were carried out in a leak tested reaction vessel, with a series of three activated carbon/alumina based solid porous media scrubbing systems, each 1 L in volume, to chemically adsorb unreacted H₂S gas.

Post-experiment, the H₂S/CO₂ stream was stopped and the system flushed with pure CO₂ to fully remove H₂S within the reaction vessel and feed lines into the scrubbers. Once safe, the reaction vessel was opened and the shaft housing the sample coupons carefully removed.

Hydrodynamic conditions

A bladed impeller was rotated at 800 RPM, necessary to create an emulsion within the reaction vessel when synthetic distillate was present. To propagate turbulence at the surface of the anti-fouling coupons, a shaft upon which they were mounted was rotated at 400 RPM, with hydrodynamic conditions represented in Table 2 representative of flow conditions within a single phase system. Rotating cylinder (RC) equipment, used extensively in corrosion and scaling research was implemented as flow becomes turbulent at very low rotational velocities, with (Re > 300) sufficient to create turbulence at the coupon surfaces¹⁴.

Table 2
Hydrodynamic conditions at sample interface

| Parameter | Value |
|--|-------|
| Reynolds number | 3376 |
| Wall shear stress (Pa) | 0.17 |
| Surface velocity (cm.s ⁻¹) | 25.1 |

Post-experimental analysis

Photographs were taken of anti-fouling coupons post-experiment (before drying), and the separation of oil/emulsion/water phases in clear vials with time. Once dried, the degree of scale deposition upon coupons was determined using gravimetric techniques, weighed on a balance with a 10µg resolution. All optical microscope pictures of o/w emulsions were then taken at x20 magnification to gauge comparative oil droplet size, mono/polydispersity and particle/surfactant presence at the droplet interface.

Electrophoretic readings of the water phase were taken using a zeta-sizer, to gauge the effect of hydrophilic polymer addition on particle charge at pH 5.2. Conductivity meter readings then determined emulsion type (oil/water or water/oil).

X-ray diffraction (XRD) analysis was carried out on dried emulsions at 0 and 500 mg/L PSI concentration to determine the crystallographic indices of uninhibited PbS species, and the effect of the polymer on count intensity and phase identification. The experiment was run with a start and stop angle of 20° and 80° respectively over a 2 hour run-time. Measurements using a rheometer with cone and plate geometry of CP 1940mm measured the viscosity of the three o/w emulsions formed at different polymer concentrations across a range of shears from 0.01 Pa to 50 Pa at 25°C.

RESULTS

Visual analysis

Figure 2 shows the degree of PbS stabilised emulsion that deposited on anti-fouling surfaces decreased with increasing PSI concentration, clearly indicated by changing of the emulsion colour from black, to brown to cream at 0, 500 and 5000 mg/L PSI respectively. Coatings F1 and F2 displayed the least fouling upon their surface at 0 mg/L, with DLC and REF showing moderate and heavy deposition respectively. A similar trend is apparent at 500 mg/L, albeit with lower levels of deposition. At a concentration of 5000 mg/L, deposition of the emulsion is uniform over all surfaces.













| Coating type | PSI concentration (mg/L) | | |
|--------------|---|--|---|
| | 0 | 500 | 5000 |
| REF |  |  |  |
| F1 |  |  |  |
| F2 |  |  |  |
| DLC |  |  |  |

Figure 2: Photographs of PbS deposition onto coatings REF, F1, F2 and DLC at PSI concentrations of 0, 500 and 5000 mg/L

Mass gain

Figure 3 shows the water contact angle vs. mass gain upon cylindrical surfaces at 0, 500 and 5000 mg/L in figures (a), (b) and (c) respectively. Significantly higher levels of deposition and mass gain were observed on hydrophilic surfaces REF and DLC at 0 mg/L PSI, compared to that seen on hydrophobic surfaces F1 and F2, where R^2 was equal to 0.89. Though mass gain upon hydrophilic surfaces was reduced significantly with the introduction of PSI at 500 mg/L, a good correlation ($R^2=0.92$) was still present between water contact angle and mass gain. Mass gain through emulsion deposition upon anti-fouling surfaces at 5000 mg/L, though limited, was uniform; hence there was no correlation between water contact angle where $R^2=0.48$.

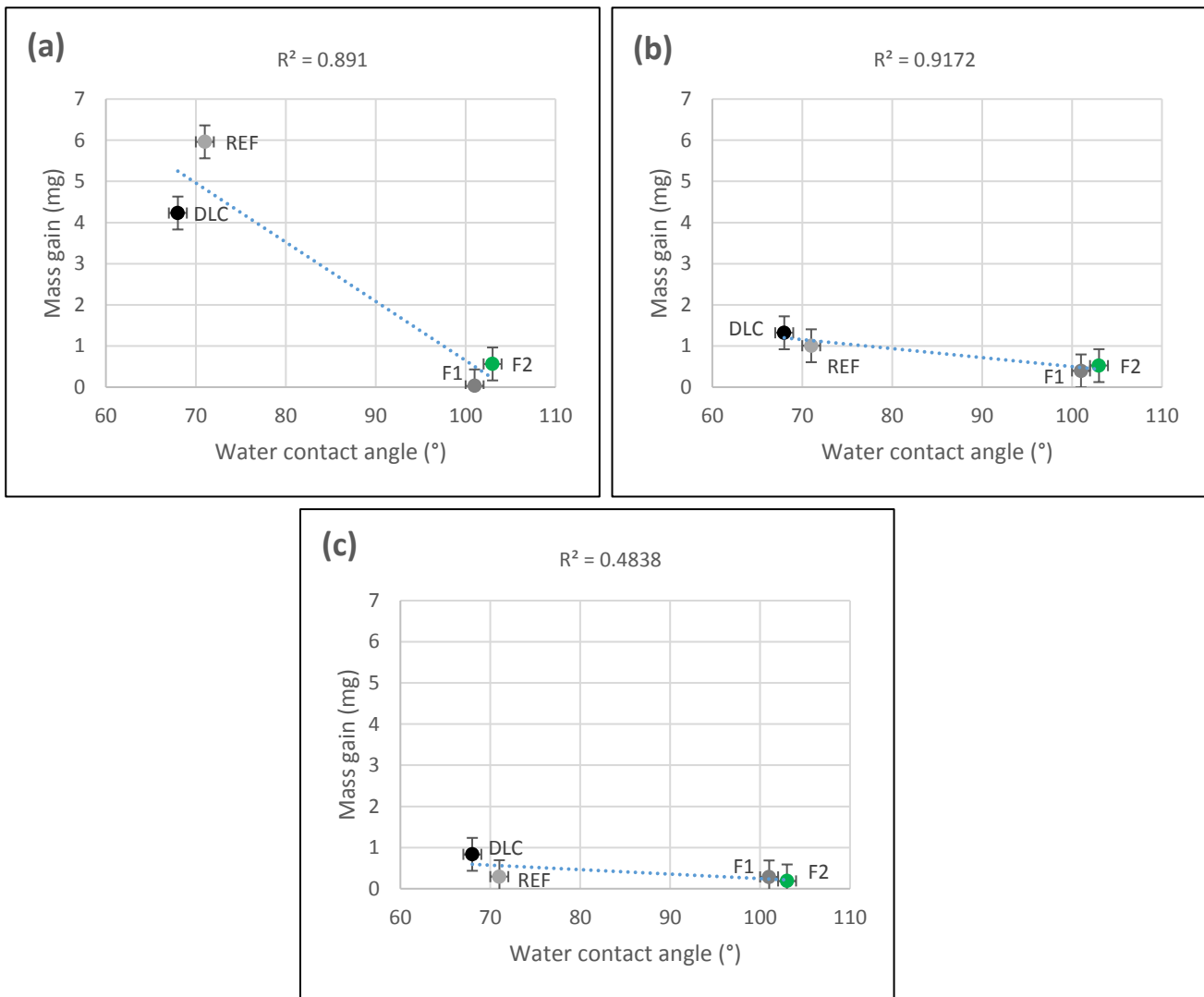


Figure 3: Water contact angle vs. Mass gain in multiphase PbS scaling environment at PSI concentrations of: (a) 0 mg/L; (b) 500 mg/L; (c) 5000 mg/L

Emulsion characterisation

When no PSI is present, the Pickering emulsion separated and stabilised into three distinct phases (oil/emulsion/water) approximately 40 seconds after agitation (Figure 4(a) & (b)). Addition of PSI at 500 mg/L and 5000 mg/L however significantly increased the time taken for the emulsion to completely stabilise, as seen in Figures 5 and 6 respectively. At 500 mg/L PSI concentration, though more stable, the oil phase was not fully emulsified, with a distinct layer present above the o/w emulsion (Figure 5(b)). At 5000 mg/L however the entire oil phase became emulsified (Figure 6(b)).

The size of oil droplets within the emulsion were generally reduced, with a rise in mono-dispersity as polymer concentration was increased. Maximum oil droplet sizes of 700, 160 and 120 microns were recorded at PSI concentrations of 0, 500 and 5000 mg/L respectively, from optical microscope images (Figures 4(c), 5(c) and 6(c)). When no polymer was present, agglomerates of PbS nanoparticles were seen to stabilise oil droplets, forming a Pickering emulsion (Figure 4(c)). When PSI was introduced to the system, negligible PbS agglomerates were visible at droplet interfaces of reduced diameter (Figures 5(c) and 6(c)).

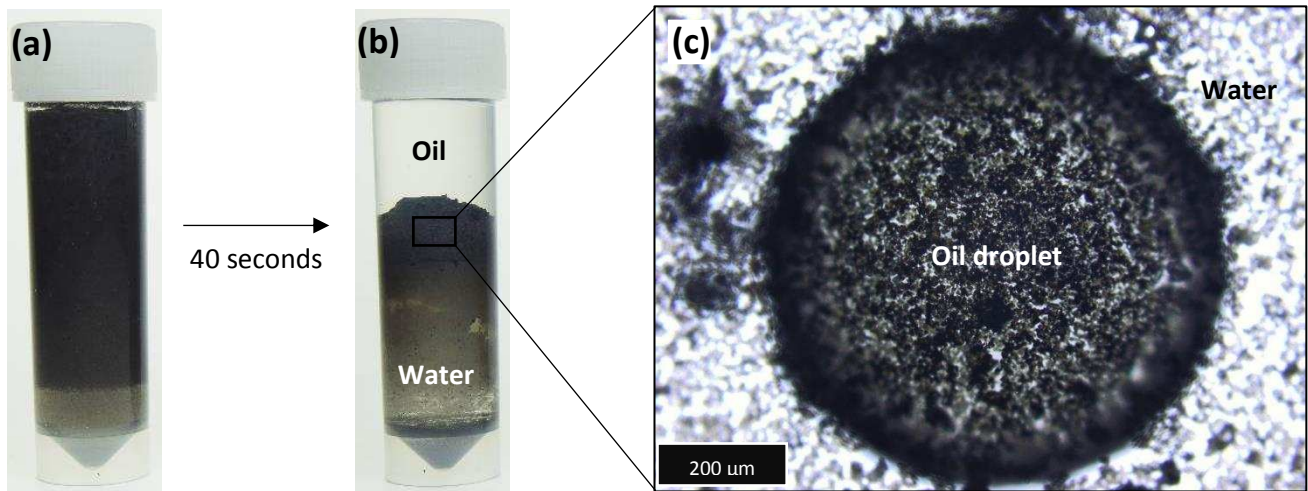


Figure 4: 0 mg/L PSI (a) Post-experimental emulsion after agitation; (b) Separation into stable 3-phase emulsion after 40 seconds; (c) Optical microscope image of oil droplet (x20 mag)

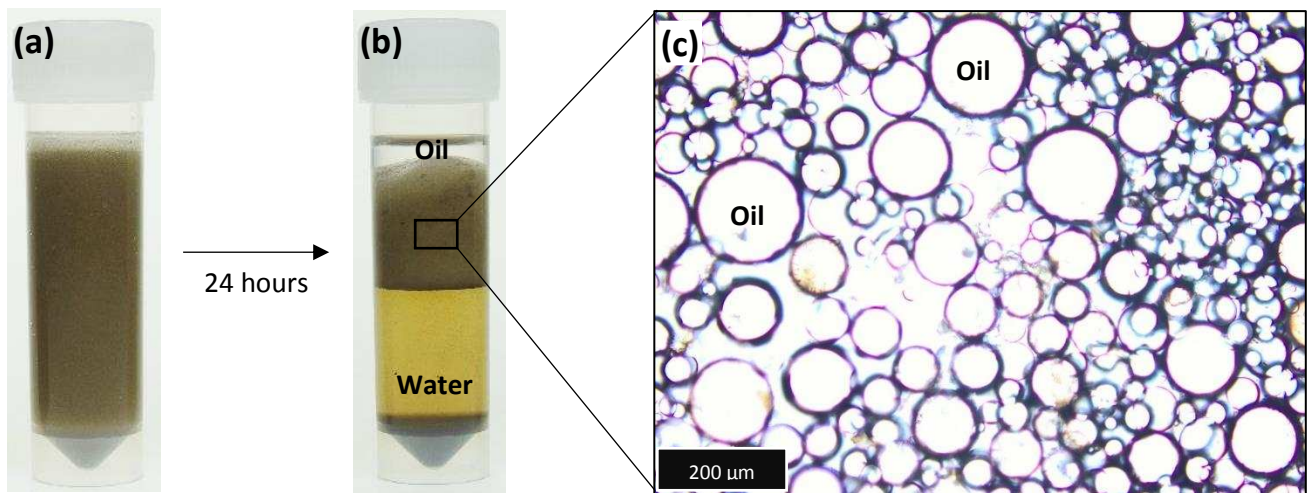


Figure 5: 500 mg/L PSI (a) Post-experimental emulsion after agitation; (b) Separation into stable 3-phase emulsion after 24 hours; (c) Optical microscope image of oil droplets (x20 mag)

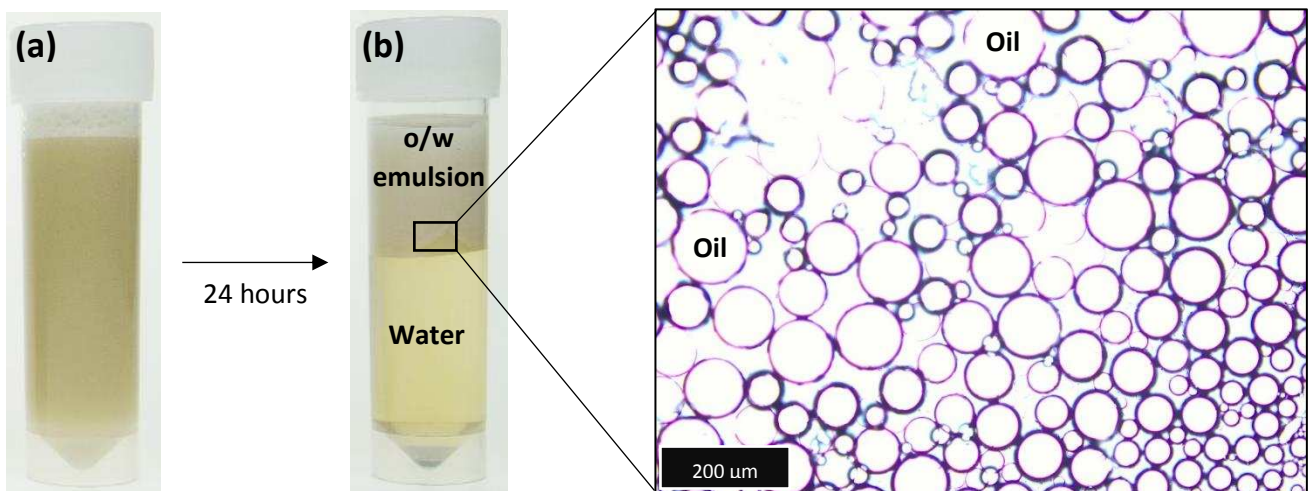


Figure 6: 5000 mg/L PSI (a) Post-experimental emulsion after agitation; (b) Separation into stable 3-phase emulsion after 24 hours; (c) Optical microscope image of oil droplets (x20 mag)

Table 3 shows the conductivity of the o/w emulsion and the zeta-potential of the aqueous brine phase post-experiment, with electrophoretic mobility seen to decrease away from the iso-electric point (I.E.P) as PSI is introduced.

Table 3
Emulsion conductivity and aqueous zeta-potential as a function of PSI concentration

| Inhibitor concentration (mg/L) | o/w emulsion conductivity (mS/cm) | Aqueous zeta-potential (mV) |
|--------------------------------|-----------------------------------|-----------------------------|
| 0 | 4.4 | -8.8 |
| 500 | 2.2 | -23.1 |
| 5000 | 3.1 | -19.4 |

XRD of emulsions

The pattern contrast of XRD spectra in Figure 7(a) and (b) shows the reduction in detectable PbS crystallographic faces, perhaps due to polymeric adsorption onto PbS at 500 mg/L PSI concentration, with a significantly lower count intensity compared to when no inhibitor is present. Distinct crystallographic planes (Miller indices) were detected at 0 mg/L where PbS is the only species formed.

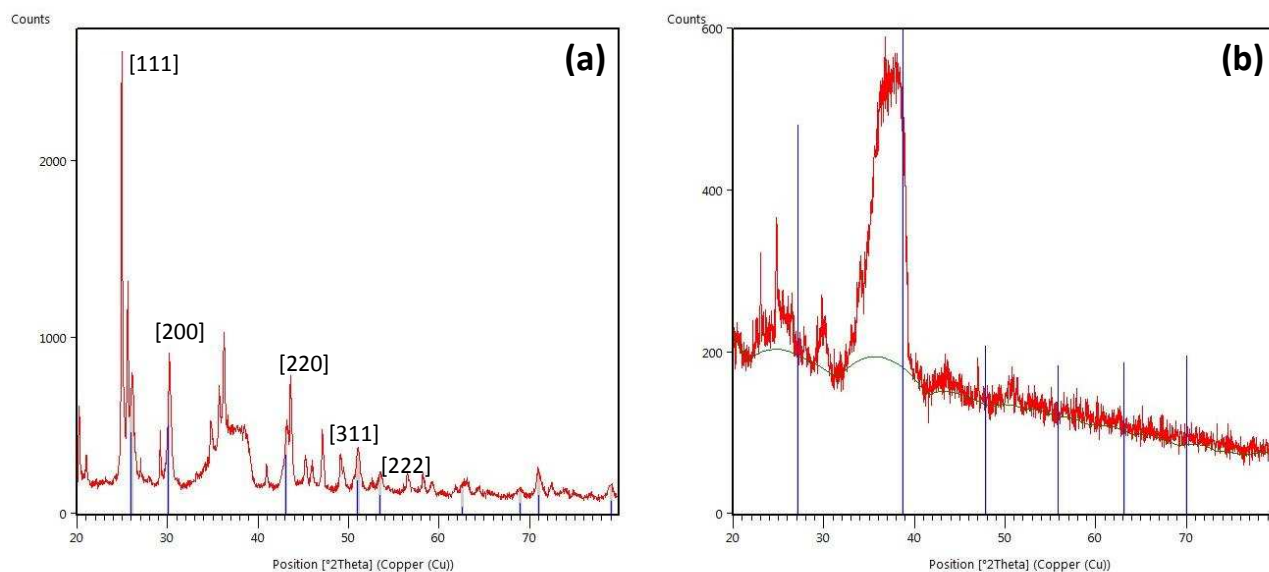


Figure 7: XRD spectra of dried O/W emulsions at PSI concentrations of: (a) 0 mg/L; (b) 500 mg/L

Emulsion viscosity

It can be seen from Figure 8 that the emulsion formed when 5000 mg/L of PSI was present required considerably higher shear stresses before droplet breaking and coalescence occurred, compared to emulsions formed at lower concentrations. At 0.17 Pa, the calculated wall shear stress at sample interfaces rotating at 400 RPM in solution, emulsion viscosities were recorded as 0.009, 0.043 and 210 Pa/s for inhibitor concentrations of 0, 500 and 5000 mg/L PSI respectively.

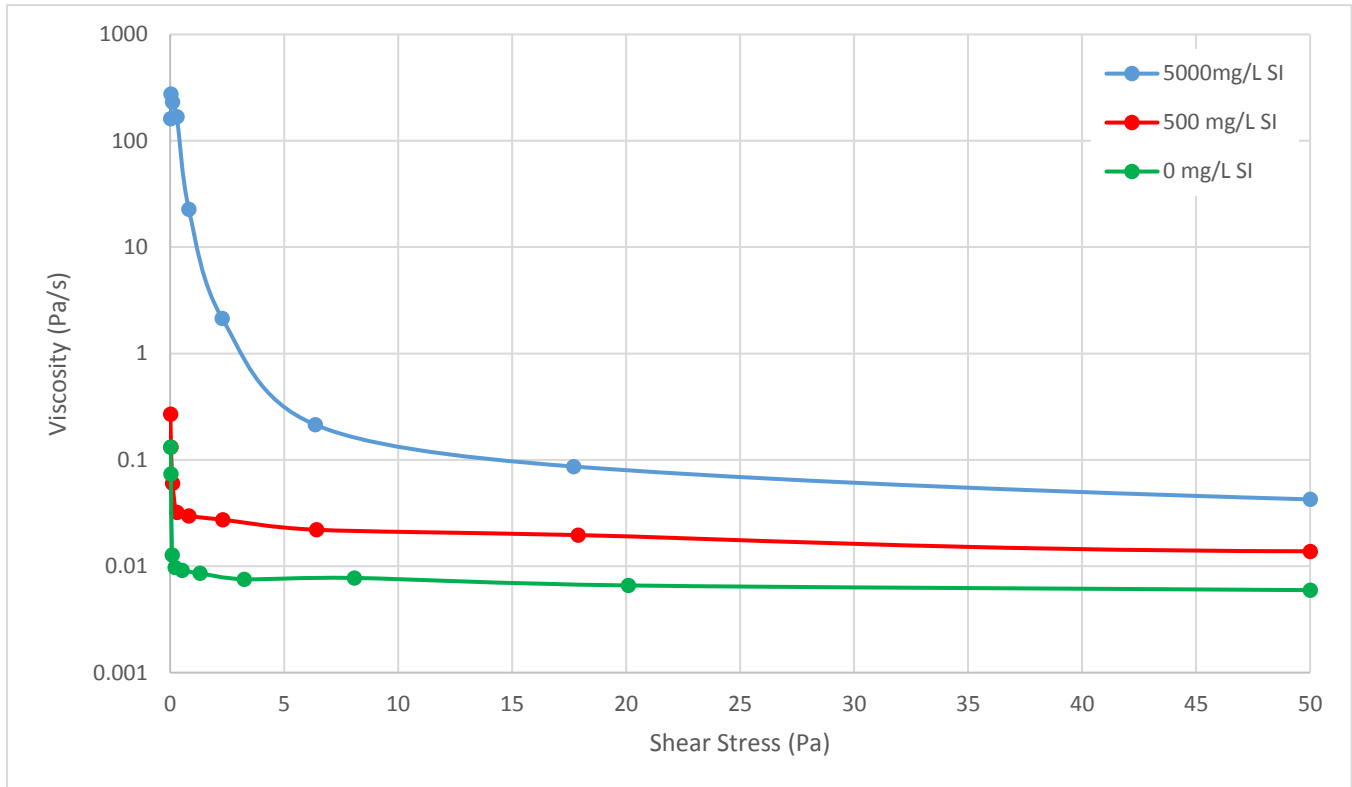


Figure 8: Shear stress (Pa) vs. Viscosity (Pa/s) of o/w emulsions at PSI concentrations of 0, 500 and 5000 mg/L

DISCUSSION

At both 0 and 500 mg/L PSI concentration, deposition was far more extensive upon hydrophilic surfaces (REF and DLC) than hydrophobic surfaces (F1 and F2), as seen in Figure 2 and Figure 3(a) and (b). As neither the concentration of solid stabilising particles or surfactant polymer was sufficient to completely emulsify the oil phase at these concentrations, a distinct oil phase was present. During scaling tests, the separated oil phase wetted hydrophobic surfaces, providing a barrier from solids adsorbed at the interface of droplets within an o/w emulsion impacting surfaces under turbulent conditions ². From Transmission Electron Microscopy (TEM) analysis, the size and morphology of o/w emulsion stabilising PbS particles and agglomerates within a system with 0 mg/L PSI present was identified (Figure 9(b) and (c)) ².

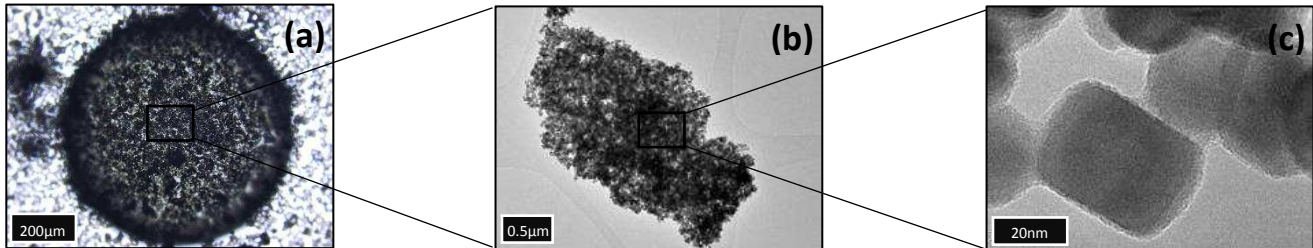


Figure 9: (a) Optical microscope - PbS stabilised oil droplet (x20 mag); (b) TEM - Agglomeration of PbS nanoparticles; (c) TEM - Individual PbS nanoparticle (cubic)

PbS nanoparticles possess intermediate hydrophobicity, with previous studies reporting clean galena particles and a clean galena surface to have an advancing contact angle (galena/water/air) of 86° and 90° respectively ^{15, 16}. As such, particles adsorbed at the o/w interface formed a mechanical barrier when no PSI was present, seen in Figure 9(a), to form a Pickering emulsion. PbS coated droplets resisted coalescence and Ostwald ripening, the latter due to an inversion in curvature at the interstices between PbS particles around smaller droplets from positive to negative, leading to maintenance of the water/particle/oil three-phase contact angle ¹⁷. Aggregation of PbS particles (Figure 9(b)) occurred due to limited electrostatic repulsion at the particle-particle electrical double layer (EDL) as stated by the DLVO theory ¹⁷, where zeta-potential of PbS particles in the aqueous phase was -8.8 mV (Table 3). PbS agglomerates heterogeneously distributed at the oil droplet interface (Figure 9(a)) likely increased the propensity for interfacial cracking under shear stress, as well as the degree of scale deposition on surfaces after droplet impaction ¹⁷.

Introduction of PSI into the system resulted in further emulsification and steric stabilisation of the oil phase (Figure 6(b)), both from adsorption onto stabilising PbS and directly at the o/w droplet interface ¹⁸. The amphiphilic nature of excess unreacted polymer resulted in interfacial adsorption between the aqueous and apolar medium, whereby the hydrophilic group extended into the aqueous phase ^{10, 19}. Though ionic complexation of Pb²⁺ with the polymer functional group likely occurred within the PbCl₂ formation water brine after PSI addition, the presence of aqueous HS⁻ anions in solution would have prompted polymer displacement. The exceedingly low solubility of PbS ($K_{sp} = 3 \times 10^{-28}$) resulted in competitive cation removal, as seen in studies detailing co-precipitation of ZnS and PbS, whereby introduction of Pb²⁺ ions to a pre-precipitated ZnS system resulted in nucleation of the thermodynamically favoured PbS ^{20, 21}.

Whilst complexation may not be the dominant inhibition mechanism in PbS forming systems, polymers have been reported to both retard nucleation and prevent further growth through lattice incorporation onto nanocrystals in the post-nucleation stage ²². AFM studies have shown surface co-ordination of polymers onto a calcite plane inhibited crystal growth in a supersaturated solution ²³. Adsorption of PSI onto precipitated PbS increased electrostatic repulsion between PbS particles at the EDL, as evidenced by a shift in measured zeta-potential from -8.8 mV to -23.1 mV at concentrations of 0 mg/L and 500 mg/L respectively (Table 3). PbS nanoparticle aggregation, typically observed at high particle concentration in uninhibited systems was thereby reduced when PSI was present, resulting in diminished depositional mass gain upon anti-fouling surfaces. The adsorption mechanism of PSI onto PbS likely varies based on PbS charge and wettability, whereby a negatively charged hydrophilic PbS surface will prompt adsorption

of the positively charged hydrophobic polymer tail, and vice versa. Migration of functionalised PbS particles to the o/w interface then leads to a reduction in interfacial tension and consequent tightening and stabilisation of the emulsion, as seen in Figures 5(c) and 6(c). Additionally, increased concentration of free amphiphiles at 5000 mg/L enhanced PSI adsorption at the o/w interface, further decreasing o/w interfacial tension²⁴. The reduction of o/w interfacial tension contributed to increased emulsion stability and viscosity, restricting movability of dispersed oil droplets, and limiting their propensity to coalesce and migrate¹⁹. Complete emulsification of the oil phase at 5000 mg/L PSI and the subsequent departure of the partitioning layer present at concentrations of 0 and 500 mg/L led to uniform deposition of viscous emulsion upon surfaces, irrespective of wettability (Figures 2 and 6(b)). Increased PSI concentration at 5000 mg/L resulted in excess free amphiphilic polymers migrating to the o/w interface, and hence had a significant effect on the viscosity and depositional behaviour of thixotropic emulsions. Under experimental conditions, shear stress at the cylindrical sample interface based on coupon geometry and hydrodynamic conditions was 0.17 Pa (Table 2). This degree of shear resulted in breaking and destabilisation of o/w emulsions formed at 0 and 500 mg/L PSI concentration, at which emulsion viscosity was recorded to be 0.009 and 0.0043 Pa/s respectively, as seen in Figure 8. When PSI concentration was increased to 5000 mg/L however, the resulting emulsion had a viscosity of 210 Pa/s at a shear stress of 0.17 Pa, approximately 5 orders of magnitude higher than that of an emulsion formed at 500 mg/L. The viscous and stable nature of the emulsion formed at 5000 mg/L PSI resulted in uniform deposition of a persistent coating on all surfaces at experimental shear values.

Whilst sample mass gain measurements indicated that deposition of solids at 5000 mg/L PSI was minimal after drying (Figure 3(c)), fouling of the nature seen in Figure 2 at 5000 mg/L within a complex and dynamic oilfield system could act as a pre-cursor to severe flow assurance issues. Solid particles within the bulk flow impinging upon surfaces layered with viscous emulsified deposits, such as the internal diameter of equipment and tubing within the production line, would be far more likely to adhere, providing sites for both crystal nucleation and further adhesion. Whilst the thickening and viscosity enhancement of o/w emulsions is sought after in chemically enhanced oil recovery (CEOR) to increase hydrocarbon yield, particularly in HT/HP applications²⁵, high surfactant polymer concentrations could prompt further deposition upon surfaces regardless of their physiochemical characteristics.

CONCLUSION

Whilst limiting the precipitation of PbS scale, introduction of excess PSI had a detrimental effect on surface fouling due to the formation of a viscous and adherent emulsion. Whilst nucleation inhibition in PbS forming systems is difficult to achieve due to low mineral solubility, adsorption of polymeric inhibitor onto the crystal surface can both retard further crystal growth and prevent precipitation. At PSI concentrations of 0 and 500 mg/L, a distinct un-emulsified oil phase acted as a barrier to adhesion of PbS stabilised o/w emulsion upon oil wet hydrophobic surfaces. However, excess PSI at concentrations of 5000 mg/L led to complete emulsification of the apolar oil phase, nullifying the advantageous effects of a partitioning oil layer. In future practices, it is recommended that amphiphilic polymer and stabilising colloidal particle levels within oilfield wells be carefully monitored and predicted in order to alleviate adhesion of viscous emulsions and precipitates upon hydrophobic downhole coatings.

Future work

Whilst PbS scale deposition poses a significant flow assurance problem in sulfide forming wells, inorganic zinc sulfide (ZnS) scales commonly form and deposit alongside PbS due to the presence of Pb^{2+} and Zn^{2+} cations in formation waters^{11, 26}. Further tests will investigate the effect of PSI concentration on ZnS precipitation and deposition onto anti-fouling surfaces; both individually and in complex PbS and ZnS forming brines.

ACKNOWLEDGEMENTS

The authors acknowledge the funding and support from the Leeds University ASSESS consortium. We also thank the financial support of the Leverhulme Trust Research Grant ECF-2016-204

REFERENCES

1. B. Eden, et al., *OILFIELD RESERVOIR SOURING*, Department of Energy, 1993.
2. W. Keogh, et al., *Evaluation of Anti-Fouling Surfaces for Prevention of Lead Sulfide Scaling in Single and Multiphase Conditions*, presented in part at CORROSION 2017, New Orleans, LA, 2017.
3. W. Keogh, et al., *Deposition of Inorganic Carbonate, Sulfate, and Sulfide Scales on Antifouling Surfaces in Multiphase Flow*, *Energy & Fuels*, 2017, 31, 11838-11851.
4. M. M. Vazirian, et al., *Surface inorganic scale formation in oil and gas industry: As adhesion and deposition processes*, *Journal of Petroleum Science and Engineering*, 2016, 137, 22-32.
5. W. Cheong, et al., *Substrate effect on surface adhesion/crystallisation of calcium carbonate*, *Journal of Crystal Growth*, 2013, 363, 7-21.
6. C. Okocha and K. Sorbie, *Scale Prediction for Iron, Zinc and Lead Sulphides and Its Relation to Scale Test Design*, 2014.
7. T. H. Lopez, et al., *Comparing efficacy of scale inhibitors for inhibition of zinc sulfide and lead sulfide scales*, 2005.
8. M. A. Barakat and E. Schmidt, *Polymer-enhanced ultrafiltration process for heavy metals removal from industrial wastewater*, *Desalination*, 2010, 256, 90-93.
9. G. A. Ilevbare, et al., *Understanding Polymer Properties Important for Crystal Growth Inhibition—Impact of Chemically Diverse Polymers on Solution Crystal Growth of Ritonavir*, *Crystal Growth & Design*, 2012, 12, 3133-3143.
10. P. Raffa, et al., *Polymeric surfactants: synthesis, properties, and links to applications*, *Chemical reviews*, 2015, 115, 8504-8563.
11. C. Okocha, et al., *Sulphide Scale (PbS/ZnS) Formation and Inhibition Tests for a Gas Condensate Field with Severe Scaling Conditions*, presented in part at SPE International, Aberdeen, United Kingdom, 2014.
12. Y. Li, et al., *Completion difficulties of HTHP and high-flowrate sour gas wells in the Longwangmiao Fm gas reservoir, Sichuan Basin, and corresponding countermeasures*, *Natural Gas Industry B*, 2016.
13. S. Ramachandran, et al., *Corrosion and Scale Formation in High Temperature Sour Gas Wells: Chemistry and Field Practice*, 2015.
14. M. Palomar-Pardave, et al., *MES 23: Electrochemistry, Nanotechnology, and Biomaterials* Electrochemical Society: Pennington, NJ, USA, 2008.
15. P. Bandini, *Surface chemical studies and heterocoagulation in metal sulphide and oxide systems*, 2000.
16. F. Bartell and G. B. Hatch, *The wetting characteristics of galena*, *The Journal of Physical Chemistry*, 1935, 39, 11-24.
17. D. J. French, *Fundamental aspects of Pickering emulsion stabilisation*, University of Edinburgh, 2016.
18. L. Payet and E. M. Terentjev, *Emulsification and stabilization mechanisms of O/W emulsions in the presence of chitosan*, *Langmuir*, 2008, 24, 12247-12252.
19. E. D. Ngouémazong, et al., *The Emulsifying and Emulsion-Stabilizing Properties of Pectin: A Review*, *Comprehensive Reviews in Food Science and Food Safety*, 2015, 14, 705-718.
20. B. G. Al-Harbi, et al., *Zinc and Lead Interactions in Combined Sulphide Scales*, 2017/4/3/, 2017.
21. H. L. Clever and F. J. Johnston, *The solubility of some sparingly soluble lead salts: an evaluation of the solubility in water and aqueous electrolyte solution*, *Journal of Physical and Chemical Reference Data*, 1980, 9, 751-784.
22. D. Patel, *Kinetics and mechanisms of crystal growth inhibition of indomethacin by model precipitation inhibitors*, University of Kentucky, 2015.
23. Q. Yang, et al., *Investigation of Calcium Carbonate Scaling Inhibition and Scale Morphology by AFM*, *Journal of Colloid and Interface Science*, 2001, 240, 608-621.
24. I. Akartuna, et al., *Stabilization of oil-in-water emulsions by colloidal particles modified with short amphiphiles*, *Langmuir*, 2008, 24, 7161-7168.
25. T. Sharma, et al., *Viscosity of the oil-in-water Pickering emulsion stabilized by surfactant-polymer and nanoparticle-surfactant-polymer system*, *Korea-Australia Rheology Journal*, 2014, 26, 377-387.
26. I. Collins and M. Jordan, *Occurance, Prediction And Prevention Of Zinc Sulfide Scale Within Gulf Coast And North Sea High Temperature/High Salinity Production Wells*, 2001.